investigate the efflux transport across the BBB since the steady-state brain concentration is governed by both the uptake and the efflux transport across the BBB.

Pitavastatin, one of the newly developed statins, contains a carboxyl acid group in its chemical structure like pravastatin. Although pitavastatin is more lipophilic than pravastatin (log $D_{7.0}$: 1.5 versus −0.47) (Ishigami et al., 2001), its brain-to-plasma concentration ratio has been reported to be lower than that of pravastatin (0.063 versus 0.48) (Komai et al., 1992; Kimata et al., 1998). The lower distribution of pitavastatin in the brain may be explained by the efflux transport across the BBB.

We have recently shown that rOat3 is expressed at the BBB (Kikuchi et al., 2003). rOat3 is a multispecific transporter, with substrates that include amphipathic organic anions as well as hydrophilic ones (Kusuhara et al., 1999). According to inhibition studies, it has been suggested that rOat3 is involved in the efflux of hydrophilic organic anions, but its contribution to the efflux transport of amphipathic organic anions, such as 17β-estradiol-D-17β-glucuronide, is limited (Sugiyama et al., 2001; Kikuchi et al., 2003). rOatp2, another multispecific organic anion transporter expressed at the BBB (Gao et al., 1999), has been suggested to account for the efflux of amphipathic organic anions across the BBB (Asaba et al., 2000; Hosoya et al., 2000; Sugiyama et al., 2001). Since pravastatin is a substrate of both rOat3 and rOatp2 (Tokui et al., 1999; Hasegawa et al., 2002), these transporters may be involved in the efflux of pravastatin and, possibly, of pitavastatin, from the brain across the BBB, accounting for the lower brain distribution of pitavastatin compared with that of pravastatin.

In the present study, we demonstrated that pravastatin and pitavastatin are substrates of both rOat3 and rOatp2 using cDNA-transfected cells. The efflux clearances of pravastatin and pitavastatin from the brain into the blood circulation across the BBB were calculated using the intracerebral microinjection technique (BEI method) and brain slice uptake experiments. In addition, the involvement of rOat3 and rOatp2 in the efflux processes was suggested in vivo by examining the inhibitory effect of several compounds.

Materials and Methods

Chemicals. [^{3}H]Pravastatin (45.5 Ci/mmol) and unlabeled pravastatin sodium [(+)-(3*R*,5*R*)-3,5-dihydroxy-7-[(1*S*,2*S*,6*S*,8*S*,8a*R*)-6-hydroxy-2-methyl-8-[(*S*)-2-methylbutyryloxyl-1,2,6,7,8,8a-hexahydro-1-naphthyl]heptanoate] were kindly donated by Sankyo (Tokyo, Japan), and [^{3}H]pitavastatin (16 Ci/mmol) and unlabeled pitavastatin [(+)-monocalcium bis[(3*R*,5*S*,6*E*)-7-[2-cyclopropyl-4-(4-fluorophenyl)-3-quinolyl]-3,5-dihydroxy-6-heptenoate] were supplied by Kowa Company Ltd. (Tokyo, Japan). [^{14}C]Carboxyl-inulin (2.5 mCi/g) was purchased from PerkinElmer Life and Analytical Sciences (Boston, MA). Unlabeled probenecid, PAH, and TCA were purchased from Sigma-Aldrich (St. Louis, MO), unlabeled digoxin was obtained from Aldrich Chemical Co. (Milwaukee, WI), and unlabeled tetraethylammonium was purchased from Wako Pure Chemicals (Osaka, Japan). Ketamine hydrochloride was purchased from Sankyo. Xylazine and ketamine hydrochloride were used as anesthetics. All other chemicals were commercially available, of reagent grade, and used without further purification.

Animals. Sprague-Dawley male rats (supplied by Japan SLC, Shizuoka, Japan) weighing 220 to 250 g were used throughout this study and had free access to food and water. All experiments using animals in this study were carried out according to the guidelines provided by the Institutional Animal Care Committee (Graduate School of Pharmaceutical Sciences, The University of Tokyo).

Transport Study. rOat3- and rOatp2-expressed LLC-PK1 cells were established and maintained as described previously (Sugiyama et al., 2001). Uptake was initiated by adding the radiolabeled ligands to the medium in the presence and absence of inhibitors after cells had been washed three times and preincubated with Krebs-Henseleit buffer at 37°C for 15 min. The Krebs-Henseleit buffer consisted of 142 mM NaCl, 23.8 mM $NaHCO_3$, 4.83 mM KCl, 0.96 mM KH_2PO_4, 1.20 mM $MgSO_4$, 12.5 mM HEPES, 5 mM glucose, and 1.53 mM $CaCl_2$ adjusted to pH 7.4. The uptake was terminated at designated times by adding ice-cold Krebs-Henseleit buffer, dissolved in 500 μl of 0.2 N NaOH and kept overnight. The radioactivity associated with the cells and medium was determined. The aliquots of cell lysate were used to determine the protein concentration by the method of Lowry (1951), with bovine serum albumin as a standard. Ligand uptake is given as the cell-to-medium concentration ratio determined as the amount of ligand associated with the cells divided by the medium concentration.

In Vivo Efflux Study. The efflux of test compounds from the brain after microinjection into the cerebral cortex was investigated using the BEI method as described previously (Kakee et al., 1996). [^{3}H]Pravastatin (15.6 nCi/rat) or [^{3}H]pitavastatin (31.3 nCi/rat) with a nonpermeable reference compound [[^{14}C]carboxyl-inulin (0.625 nCi/rat)] in 0.5 μl of ECF buffer (122 mM NaCl, 25 mM $NaHCO_3$, 10 mM D-glucose, 3 mM KCl, 1.4 mM $CaCl_2$, 1.2 mM $MgSO_4$, 0.4 mM K_2HPO_4, and 10 mM HEPES, pH 7.4) in the presence or the absence of different concentrations of various inhibitors was injected into the Par2 region (0.2 mm anterior and 5.5 mm lateral to the bregma, 4.5 mm in depth). After the microinjection, rats were decapitated, and the radioactivity that remained in the left and right cerebrum was determined. The 100-BEI (%), which represents the remaining percentage of the test compounds in the cerebrum, is described by eq. 1.

$$100 - \mathrm{BEI}\ (\%) = \frac{\dfrac{\text{amount of test drug in the brain}}{\text{amount of reference in the brain}}}{\dfrac{\text{amount of test drug injected}}{\text{amount of reference injected}}} \times 100 \quad (1)$$

The elimination rate constant of the compounds from the brain (k_{el}) was obtained by fitting the 100-BEI (%) versus time data. A nonlinear least-squares regression program (MULTI) (Yamaoka et al., 1981) was used for the calculation.

Measurement of the Distribution Volume of [^{3}H]Pravastatin and [^{3}H]Pitavastatin in the Brain. The distribution volume of pravastatin and pitavastatin in the brain was determined by the in vitro brain slice uptake technique. Brain slices were prepared as reported previously with a minor modification (Kakee et al., 1997). A hypothalamic slice, 300-μm thick, was cut using a brain microslicer (DTK-2000; Dosaka, Kyoto, Japan), and kept in oxygenated ECF buffer equilibrated with 95% O_2/5% CO_2. After preincubation for 5 min at 37°C, the brain slice (15–25 mg) was transferred to 3 ml of oxygenated incubation medium containing [^{3}H]pravastatin or [^{3}H]pitavastatin (0.05 μCi/ml) and [^{14}C]carboxyl-inulin (0.01 μCi/ml) at 37°C. At appropriate times, brain slices were collected, and the radioactivity was determined in a liquid scintillation counter. Ligand uptake was given as the amount of ligand associated with the slice divided by the medium concentration.

Results

Time Profiles of the Uptake of [^{3}H]Pravastatin and [^{3}H]Pitavastatin by cDNA-Transfected Cells. The uptake of [^{3}H]pravastatin and [^{3}H]pitavastatin by rOat3- and rOatp2-transfected LLC-PK1 cells was significantly greater than that by vector-transfected cells (Fig. 1). The uptake of pravastatin by the cDNA-transfected cells increased linearly

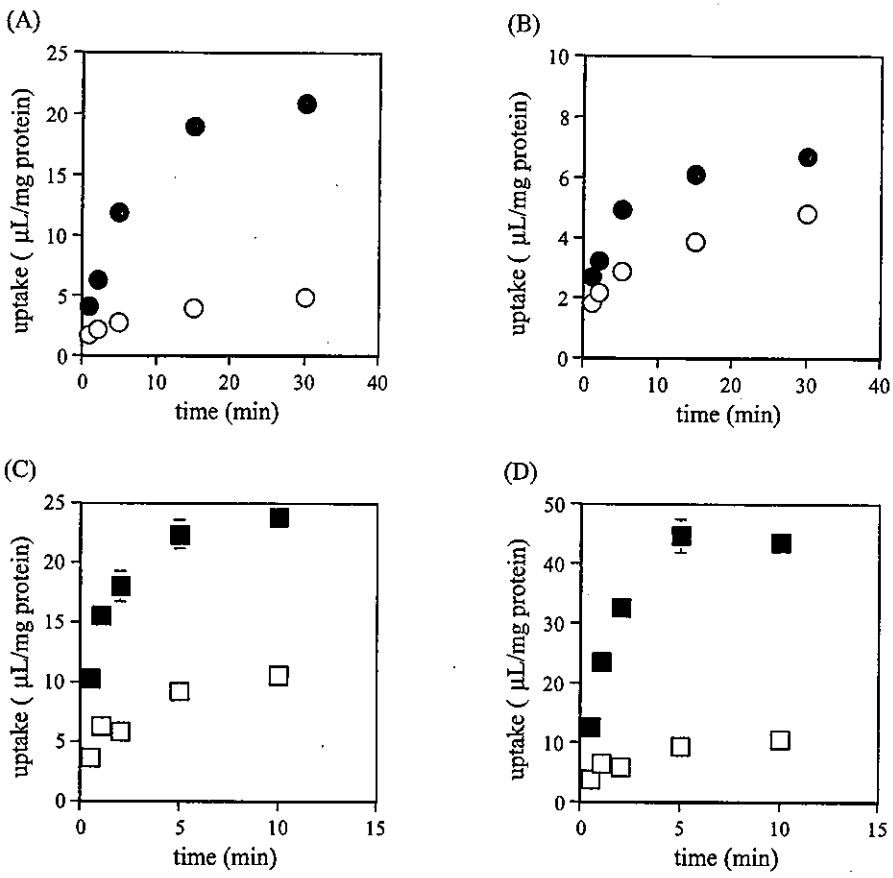

Fig. 1. Time profiles of the uptake of [^{3}H]pravastatin and [^{3}H]pitavastatin by gene-transfected LLC-PK1 cells. The uptake of [^{3}H]pravastatin (A and B) and [^{3}H]pitavastatin (C and D) by rOat3- (A and C) and rOatp2- (B and D) transfected LLC-PK1 cells was examined at 37°C. Circles and squares represent the uptake of [^{3}H]pravastatin and [^{3}H]pitavastatin, respectively. Closed and open symbols represent the uptake by gene- and vector-transfected cells, respectively. Each point represents the mean ± S.E. (n = 3).

over 5 min, whereas that of pitavastatin increased over 2 min. Eadie-Hofstee plots of the specific uptake of pitavastatin via rOat3 and rOatp2, obtained by subtracting the uptake by vector-transfected cells from that by cDNA-transfected cells, are shown in Fig. 2, A and B. Comparison of the Akaike's Information Criterion values (Yamaoka et al., 1981) suggested that the specific uptake of pitavastatin by rOat3 consists of one saturable component, and the K_m and V_{max} values of pitavastatin for rOat3 were determined as 0.982 ± 0.176 μM and 4.76 ± 0.53 pmol/min/mg protein, respectively (Fig. 2A). It was suggested that the specific uptake of pitavastatin by rOatp2 consists of one saturable and one nonsaturable component. The K_m and V_{max} values of pitavastatin for rOatp2 were 7.21 ± 0.96 μM and 80.9 ± 10.9 pmol/min/mg protein, respectively, and the uptake clearance corresponding to the nonsaturable component was 1.24 ± 0.25 μl/min/mg protein (Fig. 2B).

Time Profile of the Efflux of [^{3}H]Pravastatin and [^{3}H]Pitavastatin from the Brain across the BBB. The time profiles of the efflux of pravastatin and pitavastatin from the brain after microinjection into the cerebral cortex are shown in Fig. 3. Both statins were effluxed from the brain into the systemic circulation following microinjection, and k_{el} was calculated as 0.060 ± 0.002 min^{-1} for pravastatin and 0.026 ± 0.004 min^{-1} for pitavastatin.

Uptake of Pravastatin and Pitavastatin by Brain Slices. The distribution volume of pravastatin and pitavastatin in the brain, $V_{d,brain}$, was determined in the in vitro brain slice uptake study. Figure 4, A and B, shows the time profiles of the uptake of [^{3}H]pravastatin and [^{3}H]pitavasta-

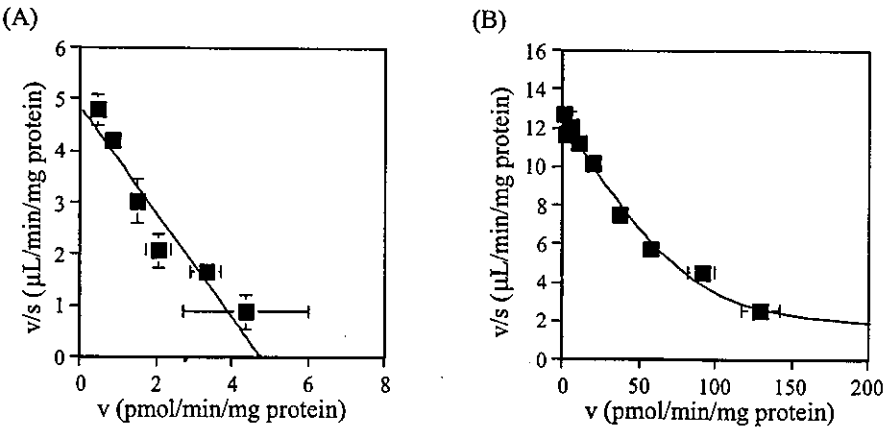

Fig. 2. Concentration dependence of the uptake of [^{3}H]pitavastatin by rOat3- and rOatp2-transfected LLC-PK1 cells. The uptake of [^{3}H]pitavastatin by rOat3- (A) and rOatp2- (B) transfected LLC-PK1 cells in the presence of unlabeled pitavastatin was examined at 37°C. Specific uptake was obtained by subtracting the uptake by vector-transfected cells from that by gene-transfected cells. The solid lines represent the fitted line obtained by nonlinear regression analysis. Each point represents the mean ± S.E. (n = 3).

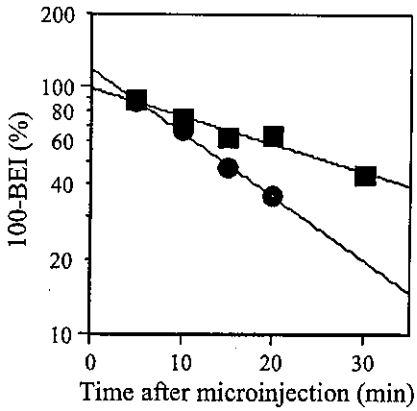

Fig. 3. Time profile of [^{3}H]pravastatin and [^{3}H]pitavastatin in the cerebrum after intracerebral microinjection. A mixture of [^{3}H]pravastatin (15.6 nCi/rat) or [^{3}H]pitavastatin (31.3 nCi/rat) and [^{14}C]carboxyl-inulin (0.625 nCi/rat) dissolved in 0.5 μl of ECF buffer was injected into Par2 of the rat cerebrum; subsequently, animals were decapitated at appropriate times. Circles and squares represent the elimination of pravastatin and pitavastatin, respectively. The solid line represents the fitted line obtained by nonlinear regression analysis. Each point represents the mean ± S.E. (n = 3).

tin by brain slices, respectively. For both statins, no significant differences in the slice-to-medium ratio between 120 and 240 min after incubation were observed, giving a steady-state slice-to-medium ratio ($V_{d,brain}$) of 0.989 ± 0.020 ml/g brain for pravastatin and 14.0 ± 0.4 ml/g brain for pitavastatin.

Calculation of the Efflux Clearances of Statins from the Brain into the Blood across the BBB. The apparent BBB efflux clearances (CL_{eff}) of pravastatin and pitavastatin were calculated by multiplying the apparent elimination rate constant (k_{el}) by the distribution volume in the brain ($V_{d,brain}$). The efflux clearances of pravastatin and pitavastatin were 59.3 ± 2.3 and 364 ± 57 μl/min/g brain, respectively.

Concentration-Dependent Efflux of Pravastatin and Pitavastatin from the Brain. The apparent elimination rate constant (k_{el}) of pravastatin and pitavastatin decreased while increasing the concentration of unlabeled substrate in the injectate (Fig. 5, A and B). Considering the dilution factor of 46.2 in the cerebrum after intracerebral microinjection (Kakee et al., 1996), the apparent Michaelis-Menten constant (K_m) for the efflux of pravastatin and pitavastatin from the brain across the BBB was estimated to be 18.2 ± 5.0 and 4.85 ± 1.14 μM, respectively.

Effect of Inhibitors on the Efflux of Statins across the BBB. The efflux of pravastatin and pitavastatin from the brain into the blood across the BBB was almost completely inhibited by 50 mM probenecid in the injectate whereas the effect of 50 mM tetraethylammonium was not significant for both statins (Fig. 6). The efflux of both statins was also inhibited by PAH, TCA, and digoxin in a concentration-dependent manner (Fig. 7).

Discussion

In the present study, the uptake of pravastatin and pitavastatin by rOat3- and rOatp2-transfected cells was determined, and the involvement of rOat3 and rOatp2 in the efflux transport across the BBB was examined.

Statins, except lovastatin and simvastatin which are administered in inactive lactone forms, are used in their active acid forms (Reinoso et al., 2002). Thus, it is possible that organic anion transporters are involved in regulating their brain concentrations. It has been shown that pravastatin is a substrate of both rOat3 and rOatp2 (Tokui et al., 1999; Hasegawa et al., 2002). Transport studies using cDNA-transfected cells demonstrated that pitavastatin is a substrate of both rOat3 and rOatp2 (Fig. 1). The transport activity of pravastatin and pitavastatin by rOat3 was comparable (Fig. 1, A and C), although the K_m value of pitavastatin (0.98 μM) was more than 10-fold smaller than that of pravastatin reported previously (13 μM) (Hasegawa et al., 2002). The transport activity of pitavastatin by rOatp2 was much greater than that of pravastatin (Fig. 1, B and D), and the K_m value of pitavastatin (7.2 μM) was approximately 5-fold smaller than that of pravastatin (38 μM) (Tokui et al., 1999). These results suggest the possibility that rOat3 and/or rOatp2 are involved in the efflux of statins from the brain across the BBB.

Pitavastatin was eliminated from the cerebral cortex more slowly than pravastatin after microinjection (Fig. 3). However, the intrinsic efflux clearance of pitavastatin from the brain across the BBB, calculated by multiplying the elimination rate constant by the distribution volume in the brain, was approximately 6-fold greater than that of pravastatin. The lower brain distribution of pitavastatin compared with that of pravastatin may be partly accounted for by the greater efflux clearance from the brain, although the difference in the uptake clearance from the blood circulation may

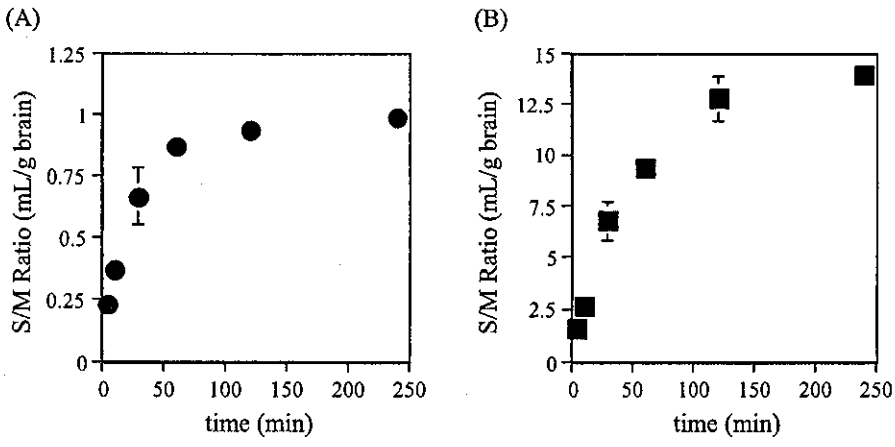

Fig. 4. Time courses of [^{3}H]pravastatin (A) and [^{3}H]pitavastatin (B) uptake by rat brain slices. Rat brain slices were incubated with 0.05 μCi/ml [^{3}H]pravastatin or [^{3}H]pitavastatin and 0.01 μCi/ml [^{14}C]carboxyl-inulin at 37°C. At appropriate times, the radioactivity in the brain slices and incubation medium was measured, and the slice-to-medium concentration ratio was estimated. Each point represents the mean ± S.E. (n = 3).

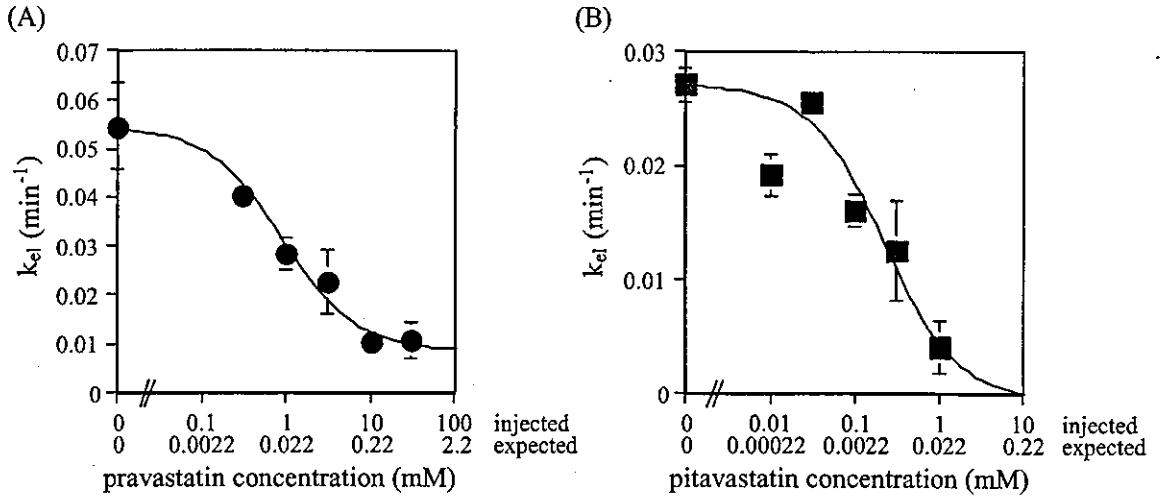

Fig. 5. Concentration dependence of the efflux of pravastatin and pitavastatin across the BBB. A, mixture of [^{3}H]pravastatin and [^{14}C]carboxyl-inulin dissolved in ECF buffer was injected into Par2 in the presence of 0, 0.3, 1, 3, 10, or 30 mM unlabeled pravastatin in the injectate. Rats were decapitated at 20 min after microinjection, and the elimination rate constant (k_{el}) was calculated. B, mixture of [^{3}H]pitavastatin and [^{14}C]carboxyl-inulin dissolved in saline was intracerebrally administered with 0, 0.01, 0.03, 0.1, 0.3, or 1 mM unlabeled pitavastatin in the injectate. Rats were decapitated at 30 min after microinjection, and the k_{el} value was calculated. Each value of the expected concentration was estimated by the concentration in the injectate divided by the dilution factor of 46.2 (Kakee et al., 1996). The solid lines represent the fitted line obtained by nonlinear regression analysis. Each point represents the mean ± S.E. (n = 3).

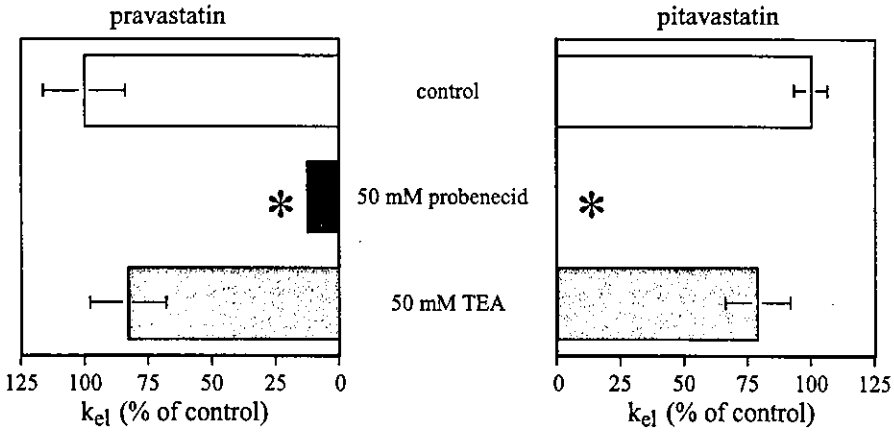

Fig. 6. Effect of unlabeled probenecid and tetraethylammonium on the efflux of [^{3}H]pravastatin (left column) or [^{3}H]pitavastatin (right column) from the cerebrum. ECF buffer containing [^{3}H]pravastatin or [^{3}H]pitavastatin and [^{14}C]carboxyl-inulin with or without unlabeled inhibitors was microinjected into Par2 of rat cerebrum, and the elimination rate constant (k_{el}) of [^{3}H]pravastatin or [^{3}H]pitavastatin was determined. The concentrations of inhibitors are shown as the injected concentration. Results are given as a ratio with respect to the elimination rate constant determined in the absence of inhibitors. Each column represents the mean ± S.E. (n = 3). *, significantly different from the control by Student's t test ($p < 0.05$).

also be one of the reasons. The efflux clearance of pravastatin was more than 3-fold greater than the previously reported uptake clearance (59 versus 18 μl/min/g brain) (Saheki et al., 1994). These results led us to conclude that there is asymmetrical transport of pravastatin across the BBB. The in vivo uptake clearance of pitavastatin into the brain may be low because of its high plasma protein binding. Thus, it is possible that the transport of pitavastatin across the BBB is also asymmetrical.

The involvement of transporters in the efflux of pravastatin and pitavastatin was investigated in vivo using the BEI method. The efflux transport of statins across the BBB was determined at different substrate concentrations. The efflux of the two statins was saturable with the saturable fraction accounting for the majority of their total efflux (Fig. 5). To obtain some insight into the transporters involved, inhibition studies were carried out. The efflux of pravastatin and pitavastatin from the brain was almost completely inhibited by the simultaneous injection of probenecid, but tetraethylammonium had no effect (Fig. 6). Furthermore, PAH (Kakee et al., 1997; Kikuchi et al., 2003) or TCA and digoxin (Kitazawa et al., 1998; Sugiyama et al., 2001) have been used as selective inhibitors for the efflux transport of hydrophilic or amphipathic organic anions across the BBB, respectively. The efflux of both statins was inhibited by these inhibitors in a concentration-dependent manner (Fig. 7). PAH inhibited the efflux of pravastatin and pitavastatin, but the inhibitory effect was partial (60% and 50%, respectively) even at the concentration sufficient to saturate its own efflux (Kakee et al., 1997; Kikuchi et al., 2003). TCA and digoxin inhibited the efflux of both statins; however, their maximum inhibitory effect differed significantly between pravastatin and pitavastatin (Fig. 7). They completely inhibited the efflux of pitavastatin, whereas their effect on the efflux of pravastatin was partial, suggesting the different contribution of the transporters involved. These results suggest that the efflux of

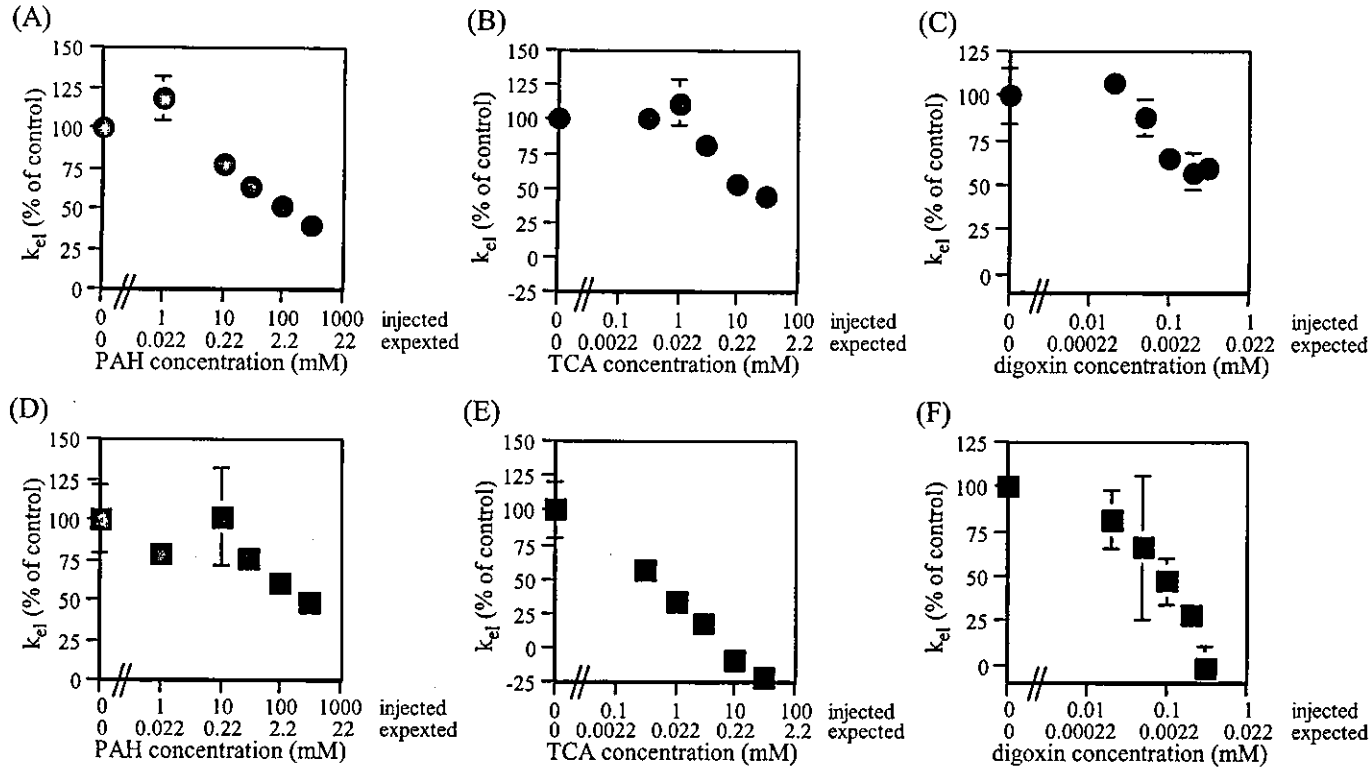

Fig. 7. Concentration dependence of the inhibitory effect of PAH, TCA, and digoxin on the efflux of [^{3}H]pravastatin or [^{3}H]pitavastatin from the cerebrum. ECF buffer containing [^{3}H]pravastatin (A–C) or [^{3}H]pitavastatin (D–F) and [^{14}C]carboxyl-inulin in the presence of different concentrations of PAH (A and D), TCA (B and E), and digoxin (C and F) was microinjected into Par2 of rat cerebrum, and k_{el} of [^{3}H]pravastatin or [^{3}H]pitavastatin was determined. Each value of the expected concentration was estimated considering the 46.2-fold dilution in the cerebrum after microinjection (Kakee et al., 1996). Results are given as a ratio with respect to the elimination rate constant determined in the absence of inhibitors. Each point represents the mean ± S.E. (n = 3).

statins consists of PAH-, TCA-, and digoxin-sensitive pathways. Since the efflux of 17β-estradiol-D-17β-glucuronide across the BBB after microinjection was completely inhibited by TCA, but partially by digoxin, the involvement of TCA-sensitive but digoxin-resistant transporters in the efflux of amphipathic organic anions has been suggested (Sugiyama et al., 2001). In the present study, TCA and digoxin inhibited the efflux of each statin to the same extent (Fig. 7). Therefore, it is likely that the TCA-sensitive but digoxin-resistant transporter(s) play a limited role in the efflux transport of statins across the BBB.

PAH has been used as an inhibitor of rOat3 (Kikuchi et al., 2003), whereas TCA has been used as an inhibitor of the amphipathic organic anion transport systems, including rOatp2, and digoxin is a specific inhibitor of rOatp2 (Sugiyama et al., 2001). The apparent K_m values of the efflux of pravastatin and pitavastatin were not very different from their K_m values for rOat3 and rOatp2: 13 and 38 μM for pravastatin (Tokui et al., 1999; Hasegawa et al., 2002), and 0.98 and 7.2 μM for pitavastatin (Fig. 2), respectively. The degree of inhibition of the efflux of pravastatin by PAH and TCA or digoxin was similar (Fig. 7, A–C) and accounted for the saturable fraction of the efflux transport. This result suggests the equal contribution of rOat3 and rOatp2 to the efflux transport of pravastatin across the BBB as high- and low-affinity sites, respectively. In the efflux transport of pitavastatin, the degree of inhibition by TCA or digoxin was greater than that by PAH (Fig. 7, D–F). However, the sum of the degree of inhibition by PAH and TCA or digoxin for the efflux of pitavastatin exceeded 100%. It is likely that these compounds inhibit other transporters at the BBB, including those expressed on the luminal membrane, since the net efflux across the BBB was evaluated by the BEI method. Assuming the PAH-sensitive fraction of the efflux of pravastatin represents the contribution of rOat3, the contribution of rOat3 to the efflux of pitavastatin across the BBB should be small since the transport activity of pitavastatin by rOat3 was similar to that of pravastatin (Fig. 1), and the intrinsic efflux clearance of pitavastatin was much greater than that of pravastatin. The difference between the transport activity of pravastatin and pitavastatin by rOatp2 may suggest a major contribution of rOatp2 to the efflux of pitavastatin across the BBB. Further studies are necessary to elucidate the transporters involved in the efflux of statins across the BBB.

Statins have been used for the drug treatment of hypercholesterolemia as inhibitors of HMG-CoA reductase. In addition to their lipid-lowering effects, increasing data suggest that these agents have properties that are potentially neuroprotective, i.e., endothelial protection via actions on the nitric oxide synthase system, as well as antioxidant, anti-inflammatory, and antiplatelet effects (Cucchiara and Kasner, 2001). Increasing the access of statins to the brain may improve their therapeutic effects in the CNS, although it may also increase the incidence of CNS side effects. The results of the present study indicate that increasing the lipophilicity is not necessarily followed by an improvement in the brain distribution, partly due to the difference in the efflux clearances from the brain. In vivo experiments such as in situ brain perfusion and the BEI method or in vitro ones using

BBB models, such as primary culture or immortalized cell lines and gene expression systems of the uptake and efflux transporters expressed at the BBB, will be required for the development of statins targeted to the CNS (Pardridge, 1998; Terasaki et al., 2003). Human OAT3 is expressed in the brain as shown by Northern blot analysis (Cha et al., 2001), and more recently, the expression of hOAT1 and hOAT3 at the choroid plexus, acting as a barrier between the blood and the cerebrospinal fluid, has been reported (Alebouyeh et al., 2003). Among the members of the human OATP family, hOATP-A has the highest homology to rOatp2 and is expressed at the BBB (Gao et al., 2000). It is possible that these human organic anion transporters play an important role in the efflux transport of organic anions across the barriers of the CNS. Their cDNA-transfected cells will provide screening systems for statins and other candidate drugs with anionic moieties.

In conclusion, both pravastatin and pitavastatin undergo efflux from the brain into the blood across the BBB, and at least two transporters, rOat3 and rOatp2, are involved in the efflux processes, each making a different contribution. It is likely that one of the underlying mechanisms of the lower brain distribution of pitavastatin compared with pravastatin despite its higher lipophilicity is the difference in the efflux transport clearance, i.e., in the transport activity by rOatp2.

Acknowledgments

We thank Sankyo (Tokyo, Japan) for providing labeled and unlabeled pravastatin and Kowa Company Ltd. (Tokyo, Japan) for providing labeled and unlabeled pitavastatin.

References

Alebouyeh M, Takeda M, Onozato ML, Tojo A, Noshiro R, Hasannejad H, Inatomi J, Narikawa S, Huang XL, Khamdang S, et al. (2003) Expression of human organic anion transporters in the choroid plexus and their interactions with neurotransmitter metabolites. *J Pharmacol Sci* **93**:430–436.

Asaba H, Hosoya K, Takanaga H, Ohtsuki S, Tamura E, Takizawa T, and Terasaki T (2000) Blood-brain barrier is involved in the efflux transport of a neuroactive steroid, dehydroepiandrosterone sulfate, via organic anion transporting polypeptide 2. *J Neurochem* **75**:1907–1916.

Barth JD, Kruisbrink OA, and Van Dijk AL (1990) Inhibitors of hydroxymethylglutaryl coenzyme A reductase for treating hypercholesterolaemia. *BMJ* **301**:669.

Cha SH, Sekine T, Fukushima JI, Kanai Y, Kobayashi Y, Goya T, and Endou H (2001) Identification and characterization of human organic anion transporter 3 expressing predominantly in the kidney. *Mol Pharmacol* **59**:1277–1286.

Cucchiara B and Kasner SE (2001) Use of statins in CNS disorders. *J Neurol Sci* **187**:81–89.

Gao B, Hagenbuch B, Kullak-Ublick GA, Benke D, Aguzzi A, and Meier PJ (2000) Organic anion-transporting polypeptides mediate transport of opioid peptides across blood-brain barrier. *J Pharmacol Exp Ther* **294**:73–79.

Gao B, Stieger B, Noe B, Fritschy JM, and Meier PJ (1999) Localization of the organic anion transporting polypeptide 2 (Oatp2) in capillary endothelium and choroid plexus epithelium of rat brain. *J Histochem Cytochem* **47**:1255–1264.

Golden PL and Pollack GM (2003) Blood-brain barrier efflux transport. *J Pharm Sci* **92**:1739–1753.

Hasegawa M, Kusuhara H, Sugiyama D, Ito K, Ueda S, Endou H, and Sugiyama Y (2002) Functional involvement of rat organic anion transporter 3 (rOat3; Slc22a8) in the renal uptake of organic anions. *J Pharmacol Exp Ther* **300**:746–753.

Hosoya K, Asaba H, and Terasaki T (2000) Brain-to-blood efflux transport of estrone-3-sulfate at the blood-brain barrier in rats. *Life Sci* **67**:2699–2711.

Ishigami M, Honda T, Takasaki W, Ikeda T, Komai T, Ito K, and Sugiyama Y (2001) A comparison of the effects of 3-hydroxy-3-methylglutaryl-coenzyme a (HMG-CoA) reductase inhibitors on the CYP3A4-dependent oxidation of mexazolam in vitro. *Drug Metab Dispos* **29**:282–288.

Kakee A, Terasaki T, and Sugiyama Y (1996) Brain efflux index as a novel method of analyzing efflux transport at the blood-brain barrier. *J Pharmacol Exp Ther* **277**:1550–1559.

Kakee A, Terasaki T, and Sugiyama Y (1997) Selective brain to blood efflux transport of para-aminohippuric acid across the blood-brain barrier: in vivo evidence by use of the brain efflux index method. *J Pharmacol Exp Ther* **283**:1018–1025.

Kikuchi R, Kusuhara H, Sugiyama D, and Sugiyama Y (2003) Contribution of organic anion transporter 3 (Slc22a8) to the elimination of *p*-aminohippuric acid and benzylpenicillin across the blood-brain barrier. *J Pharmacol Exp Ther* **306**: 51–58.

Kimata H, Fujino H, Koide T, Yamada Y, Tsunenari Y, and Yanagawa Y (1998) Studies on the metabolic fate of NK-104, a new inhibitor of HMG-CoA reductase: I. Absorption, distribution, metabolism and excretion in rats. *Xenobiol Metabol Dispos* **13**:484–498.

Kitazawa T, Terasaki T, Suzuki H, Kakee A, and Sugiyama Y (1998) Efflux of taurocholic acid across the blood-brain barrier: interaction with cyclic peptides. *J Pharmacol Exp Ther* **286**:890–895.

Komai T, Kawai K, Tokui T, Tokui Y, Kuroiwa C, Shigehara E, and Tanaka M (1992) Disposition and metabolism of pravastatin sodium in rats, dogs and monkeys. *Eur J Drug Metab Pharmacokinet* **17**:103–113.

Kusuhara H, Sekine T, Utsunomiya-Tate N, Tsuda M, Kojima R, Cha SH, Sugiyama Y, Kanai Y, and Endou H (1999) Molecular cloning and characterization of a new multispecific organic anion transporter from rat brain. *J Biol Chem* **274**:13675–13680.

Kusuhara H and Sugiyama Y (2001a) Efflux transport systems for drugs at the blood-brain barrier and blood-cerebrospinal fluid barrier (part 1). *Drug Discov Today* **6**:150–156.

Kusuhara H and Sugiyama Y (2001b) Efflux transport systems for drugs at the blood-brain barrier and blood-cerebrospinal fluid barrier (part 2). *Drug Discov Today* **6**:206–212.

Kusuhara H, Suzuki H, Terasaki T, Kakee A, Lemaire M, and Sugiyama Y (1997) P-Glycoprotein mediates the efflux of quinidine across the blood-brain barrier. *J Pharmacol Exp Ther* **283**:574–580.

Lee G, Dallas S, Hong M, and Bendayan R (2001) Drug transporters in the central nervous system: brain barriers and brain parenchyma considerations. *Pharmacol Rev* **53**:569–596.

Lowry O (1951) Protein measurement with the Folin phenol reagent. *J Biol Chem* **193**:265–273.

Ohtsuki S, Asaba H, Takanaga H, Deguchi T, Hosoya K, Otagiri M, and Terasaki T (2002) Role of blood-brain barrier organic anion transporter 3 (OAT3) in the efflux of indoxyl sulfate, a uremic toxin: its involvement in neurotransmitter metabolite clearance from the brain. *J Neurochem* **83**:57–66.

Pardridge WM (1998) CNS drug design based on principles of blood-brain barrier transport. *J Neurochem* **70**:1781–1792.

Reinoso RF, Sanchez Navarro A, Garcia MJ, and Prous JR (2002) Preclinical pharmacokinetics of statins. *Methods Find Exp Clin Pharmacol* **24**:593–613.

Saheki A, Terasaki T, Tamai I, and Tsuji A (1994) In vivo and in vitro blood-brain barrier transport of 3-hydroxy-3-methylglutaryl coenzyme A (HMG-CoA) reductase inhibitors. *Pharm Res (NY)* **11**:305–311.

Schaefer EJ (1988) HMG-CoA reductase inhibitors for hypercholesterolemia. *N Engl J Med* **319**:1222–1223.

Sugiyama D, Kusuhara H, Lee YJ, and Sugiyama Y (2003) Involvement of multidrug resistance associated protein 1 (Mrp1) in the efflux transport of 17beta estradiol-D-17beta-glucuronide (E217betaG) across the blood-brain barrier. *Pharm Res (NY)* **20**:1394–1400.

Sugiyama D, Kusuhara H, Shitara Y, Abe T, Meier PJ, Sekine T, Endou H, Suzuki H, and Sugiyama Y (2001) Characterization of the efflux transport of 17beta-estradiol-D-17beta- glucuronide from the brain across the blood-brain barrier. *J Pharmacol Exp Ther* **298**:316–322.

Sun H, Dai H, Shaik N, and Elmquist WF (2003) Drug efflux transporters in the CNS. *Adv Drug Deliv Rev* **55**:83–105.

Terasaki T, Ohtsuki S, Hori S, Takanaga H, Nakashima E, and Hosoya K (2003) New approaches to in vitro models of blood-brain barrier drug transport. *Drug Discov Today* **8**:944–954.

Tokui T, Nakai D, Nakagomi R, Yawo H, Abe T, and Sugiyama Y (1999) Pravastatin, an HMG-CoA reductase inhibitor, is transported by rat organic anion transporting polypeptide, oatp2. *Pharm Res (NY)* **16**:904–908.

Yamaoka K, Tanigawara Y, Nakagawa T, and Uno T (1981) A pharmacokinetic analysis program (multi) for microcomputer. *J Pharmacobiodyn* **4**:879–885.

Address correspondence to: Yuichi Sugiyama, Department of Molecular Pharmacokinetics, Graduate School of Pharmaceutical Sciences, The University of Tokyo, 7-3-1 Hongo, Bunkyo-ku, Tokyo 113-0033, Japan. E-mail: sugiyama@mol.f.u-tokyo.ac.jp

5 Oct 2004 :1308 AR AR232-PA45-28.tex XMLPublish[SM](2004/02/24) P1: JRX
AR REVIEWS IN ADVANCE10.1146/annurev.pharmtox.44.101802.121444
(Some corrections may occur before final publication online and in print)

Annu. Rev. Pharmacol. Toxicol. 2005. 45:689–723
doi: 10.1146/annurev.pharmtox.44.101802.121444

First published online as a Review in Advance on October 12, 2004

EVALUATION OF DRUG-DRUG INTERACTION IN THE HEPATOBILIARY AND RENAL TRANSPORT OF DRUGS

Yoshihisa Shitara,[1] Hitoshi Sato,[1] and Yuichi Sugiyama[2]
[1]*School of Pharmaceutical Sciences, Showa University, Shinagawa-ku, Tokyo 142-8555, Japan; email: shitara@pharm.showa-u.ac.jp, satohito@pharm.showa-u.ac.jp*
[2]*Graduate School of Pharmaceutical Sciences, University of Tokyo, Bunkyo-ku, Tokyo 113-0033, Japan; email: sugiyama@mol.f.u-tokyo.ac.jp*

Key Words transporter, pharmacokinetics, quantitative prediction of drug-drug interaction

■ **Abstract** Recent studies have revealed the import role played by transporters in the renal and hepatobiliary excretion of many drugs. These transporters exhibit a broad substrate specificity with a degree of overlap, suggesting the possibility of transporter-mediated drug-drug interactions with other substrates. This review is an overview of the roles of transporters and the possibility of transporter-mediated drug-drug interactions. Among the large number of transporters, we compare the K_i values of inhibitors for organic anion transporting polypeptides (OATPs) and organic anion transporters (OATs) and their therapeutic unbound concentrations. Among them, cephalosporins and probenecid have the potential to produce clinically relevant OAT-mediated drug-drug interactions, whereas cyclosporin A and rifampicin may trigger OATP-mediated ones. These drugs have been reported to cause drug-drug interactions in vivo with OATs or OATPs substrates, suggesting the possibility of transporter-mediated drug-drug interactions. To avoid adverse consequences of such transporter-mediated drug-drug interactions, we need to be more aware of the role played by drug transporters as well as those caused by drug metabolizing enzymes.

INTRODUCTION

The kidney and the liver play important roles in the elimination of drugs and xenobiotics from the body (1–5). Cumulative in vivo and in vitro studies have revealed the importance of transporters in the renal and hepatobiliary excretion of many drugs and other xenobiotics (1–5). Recent studies to investigate the molecular mechanism of renal and hepatobiliary excretion have revealed that multiple transporters are expressed in the kidney and liver in animals and humans, as well as revealing their function, tissue distribution, and intracellular localization (6–15). These transporters exhibit broad substrate specificity with a degree of overlap.

5 Oct 2004 :1308 AR AR232-PA45-28.tex XMLPublish^{SM}(2004/02/24) P1: JRX
AR REVIEWS IN ADVANCE10.1146/annurev.pharmtox.44.101802.121444

As each transporter accepts multiple drugs and/or xenobiotics as its substrates, it may be competitively inhibited by other coadministered drugs and/or xenobiotics, which may lead to drug-drug interactions involving the transporter (15, 16). In this review, we summarize quantitatively the probability of drug-drug interactions from in vitro and in vivo studies.

THE MECHANISM OF RENAL AND HEPATOBILIARY EXCRETION OF DRUGS

The Mechanism of Renal Excretion—The Role of Transporters

In the kidney, drugs are excreted in the urine as the net result of glomerular filtration, tubular secretion, and reabsorption (4) (Figure 1). The mechanism of glomerular filtration is simply ultrafiltration of drugs and xenobiotics, which do not bind to macromolecules such as plasma proteins, and, therefore, transporters are not involved in this process. Therefore, for drugs eliminated only by filtration, renal excretion is not saturable and cannot be inhibited by other drugs. On the other hand, in the case of tubular secretion, several active secretion mechanisms have been reported in the proximal tubules, which are mainly mediated by transporters.

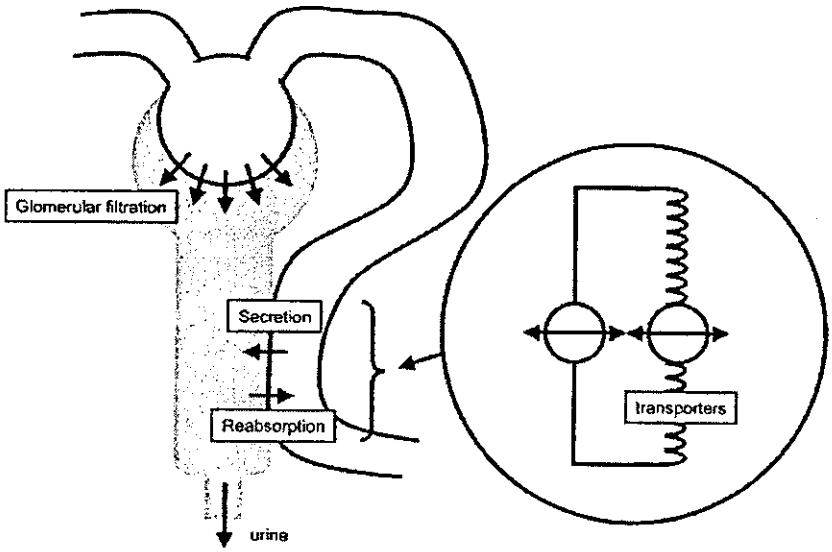

Figure 1 Mechanism of drug elimination in the kidney. Drug elimination in the kidney takes place by glomerular filtration and secretion at the proximal tubules. However, they may return to the systemic circulation via a process of drug reabsorption. Transporters are involved in drug secretion and reabsorption.

Hence, this process is saturable and may be inhibited by coadministered drugs. As with tubular secretion, the reabsorption process is sometimes mediated by transporters in the proximal tubules. Therefore, the reabsorption process may be, in part, saturable and inhibited by coadministered drugs. Renal clearance can be, in general, described by the following equation:

$$CL_R = (1 - FR) \cdot (f_u \cdot GFR + CL_{scc})$$
$$= (1 - FR) \cdot \left(f_u \cdot GFR + \frac{Q_R \cdot f_u \cdot CL_{R,int}}{Q_R + f_u \cdot CL_{R,int}} \right), \quad 1.$$

where f_u, GFR, FR, CL_{scc}, Q_R, and $CL_{R,int}$ represent protein unbound fraction in the blood, glomerular filtration rate [ml min^{-1}], the fraction reabsorbed, renal secretion clearance, renal blood flow rate, and intrinsic clearance of tubular secretion, respectively (4). FR and $CL_{R,int}$ are partly saturable and can be inhibited, suggesting the possibility of drug-drug interactions.

The Mechanism of Hepatobiliary Excretion—The Role of Transporters

In the liver, drugs are first taken up into hepatocytes, followed by metabolism including oxidation (mediated by cytochrome P450, Phase I) and conjugation (mediated by conjugation enzymes, Phase II), and excreted into the bile (Phase III) (3) (Figure 2). Some drugs are excreted as intact drugs without metabolism. In addition, drugs excreted in the intact form may pass into the blood again by enterohepatic circulation. Drugs or their metabolites, once taken up into the liver, may undergo secretion into the blood across the sinusoidal membrane, followed by the hepatobiliary or renal excretion. To date, transporters have been shown to play a role in hepatic uptake, biliary excretion, and the secretion into the blood across the sinusoidal membrane (Figure 2). Hepatic clearance can be described by the following equation (17, 18):

$$CL_H = \frac{Q_H \cdot f_u \cdot CL_{H,int,all}}{Q_H + f_u \cdot CL_{H,int,all}}, \quad 2.$$

where CL_H, Q_H, and $CL_{H,int,all}$ represent the hepatic clearance; hepatic blood flow; and overall intrinsic clearance of biliary excretion, including uptake, metabolism, and biliary excretion, respectively. $CL_{H,int,all}$ can be described by the following equation (3, 19):

$$CL_{H,int,all} = PS_{influx} \times \frac{CL_{H,int}}{PS_{efflux} + CL_{H,int}}, \quad 3.$$

where PS_{influx} and PS_{efflux} are the membrane permeability across the sinusoidal membrane from the outside to the inside and from the inside to the outside of cells, respectively, and $CL_{H,int}$ represents the exact intrinsic clearance for the metabolism and/or biliary excretion of the unbound drugs. When $CL_{H,int}$ is negligibly low

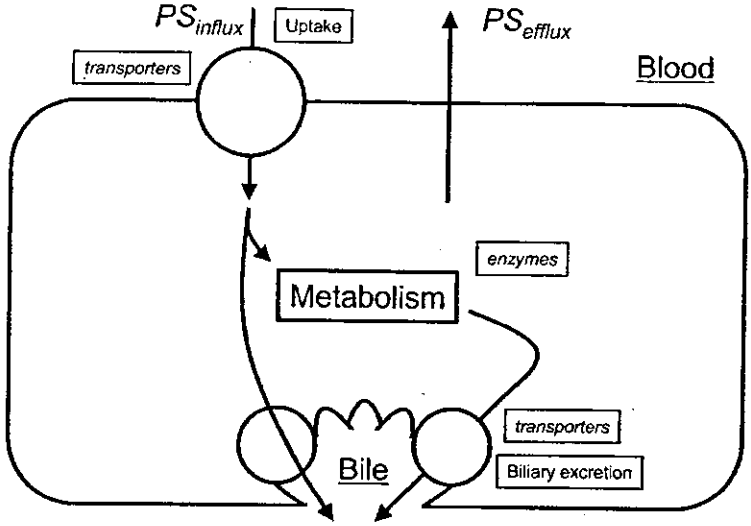

Figure 2 Mechanism of drug elimination in the liver. Drugs are taken up into hepatocytes via transporters and/or passive diffusion, followed by metabolism and/or biliary excretion. Drugs are possibly effluxed into the circulation via sinusoidal membrane.

compared with PS_{efflux} ($CL_{H,int} \ll PS_{efflux}$), Equation 3 gives

$$CL_{H,int,all} = PS_{influx} \times \frac{CL_{H,int}}{PS_{efflux}}. \quad 4.$$

If PS_{efflux} is much lower than $CL_{H,int}$ ($CL_{H,int} \gg PS_{efflux}$), Equation 3 gives

$$CL_{H,int,all} = PS_{influx}. \quad 5.$$

It should be noted that the uptake of drugs via the sinusoidal membrane (PS_{influx}), which is partly mediated by transporters, is a determinant of the net hepatic clearance regardless of the other processes, i.e., $CL_{H,int}$ and PS_{efflux}. Therefore, hepatic clearance may be affected when the uptake clearance of drugs is altered, even if the drug finally undergoes metabolism. On the other hand, the excretion of drugs via the bile canalicular membrane, which is partly mediated by transporters, is a determinant of the net hepatic clearance, unless PS_{efflux} is negligibly low compared with $CL_{H,int}$. Therefore, except in this case, the change in the biliary excretion may affect the net hepatic clearance. If PS_{efflux} is much lower than $CL_{H,int}$, only a drastic reduction in the biliary excretion will affect the net hepatic clearance, possibly leading to a transporter-mediated drug-drug interaction.

5 Oct 2004 :1308 AR AR232-PA45-28.tex XMLPublish^{SM}(2004/02/24) P1: JRX
AR REVIEWS IN ADVANCE10.1146/annurev.pharmtox.44.101802.121444

TRANSPORTERS IN THE KIDNEY AND LIVER

Recently, many types of transporters have been isolated in the kidney and liver from animals and humans. Their substrate specificity has been characterized using cRNA-injected oocytes and/or cDNA transfected cells. Generally, amphipathic organic anions with relatively high molecular weights are eliminated from the liver by metabolism and/or biliary excretion, whereas small and hydrophilic organic anions are excreted into urine (7). In this section, the characteristics of transporters expressed in the kidney and liver and their functions are summarized.

Transporters in the Kidney

Figure 3 shows transporters expressed in the kidney of rats and humans. Some transporters are located on the basolateral membrane (blood side), whereas others are located on the brush border membrane (luminal side), and these transporters contribute to membrane transport, resulting in tubular secretion and/or reabsorption. In this section, the molecular aspects of renal transporters are summarized.

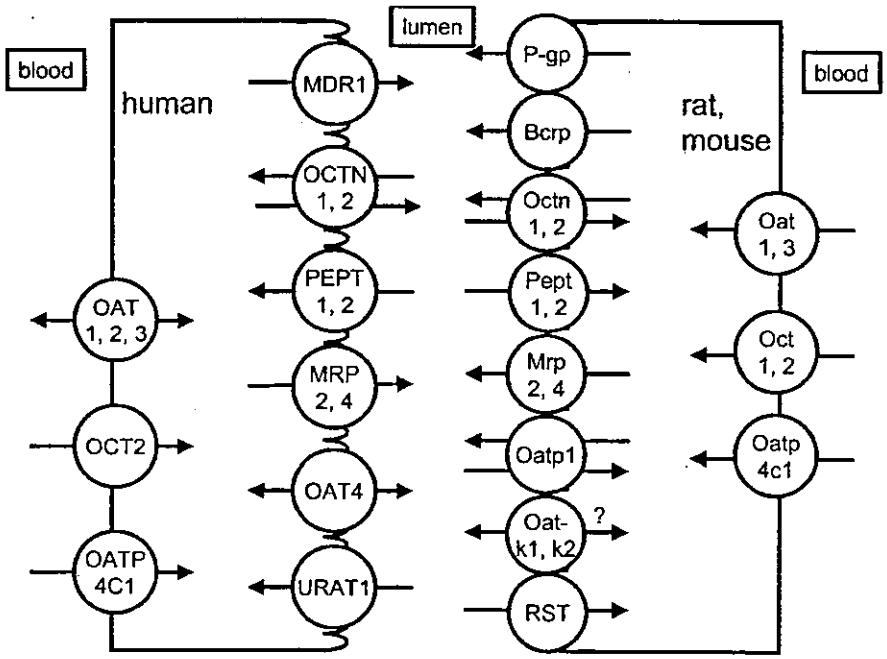

Figure 3 Transporters in the kidney. Transporters expressed in human and rodent kidney are summarized in this figure. Some of the transporters in rodents are expressed only in either rats or mice.

ORGANIC ANION TRANSPORTERS The transport of organic anions is mainly mediated by organic anion transporters (OATs). Rat Oat1 has been isolated as a renal transporter that is involved in the renal uptake of organic anions like p-aminohippuric acid (PAH) in an exchange of dicarboxylates (20). OAT1–5 have been identified as human OAT family transporters (21–24). Among them, OAT1–4 are expressed in the human kidney and OAT2 and 5 are expressed in the liver (21–24). In the kidney, OAT1–3 are localized on the basolateral membrane, whereas OAT4 is localized on the brush border membrane (24). Each of these transporters in the OAT family has a similar substrate specificity. These transporters accept organic anions with a relatively small molecular weight with some exceptions. They accept PAH, methotrexate (MTX), nonsteroidal antiinflammatory drugs, and antiviral nucleoside analogues as substrates (25–27). They also accept more lipophilic organic anions, such as estrone 3-sulfate and ochratoxin A, and even an organic cation, cimetidine (24, 25, 28).

P-GLYCOPROTEIN P-glycoprotein (P-gp) consists of two subclasses: MDR1 (MDR1 in humans, Mdr1a and 1b in rats and mice) and MDR2 [MDR2 (or 3) in humans and Mdr2 in rats and mice] (8). The former is the well-known multidrug resistance transporter, whereas the latter is a translocator for phospholipids (8). In the kidney, P-gp is localized on the brush border membrane and acts as an efflux transporter into the urine (8). P-gp is also expressed in the liver (8). In the liver, it is localized on the bile canalicular membrane (8). P-gp was originally found as an overexpressing transporter in tumor tissues, and it acts as a multidrug resistance protein, although it has also been identified in normal tissues such as kidney, liver, blood-brain barrier, and intestine (8). P-gp substrates include anticancer drugs (such as vincristine, vinblastine, doxorubicin, daunorubicin, etoposide, and paclitaxel), immunosuppresants (such as cyclosporin A), verapamil, digoxin, and steroids (such as aldosterone and cortisole) (29–36).

PEPTIDE TRANSPORTERS In the kidney, two isoforms of peptide transporters have been identified: PEPT1 and PEPT2 (37). PEPT1 and 2 are localized on the brush border membrane of the proximal tubule (38, 39). PEPT1 is expressed in the early part of the proximal tubule (pars convoluta), whereas PEPT2 is expressed further along the proximal tubule (pars recta) (38, 39). PEPT1 and 2 accept not only di- or tri-peptides but also several therapeutic drugs. PEPT1 accepts therapeutic drugs such as β-lactam antibiotics (such as cephalexin, ceftibuten, cephradine), ACE inhibitors (enalapril and temocapril), and valacyclovir (37, 40, 41). Although there are few therapeutic drugs that have been reported to be substrates of PEPT2 (cephalexin), there are many drugs that interact with PEPT2 as inhibitors (37).

ORGANIC CATION TRANSPORTERS OCT1 and OCT2 are expressed in the kidney, whereas only OCT1 is expressed in the liver (14, 42). OCT2 is highly expressed in the kidney (14, 42). In human kidney, these transporters are localized in the basolateral membrane and are important organic cation transporters for renal

5 Oct 2004 :1308 AR AR232-PA45-28.tex XMLPublish^{SM}(2004/02/24) P1: JRX
AR REVIEWS IN ADVANCE10.1146/annurev.pharmtox.44.101802.121444

tubular secretion (14, 42). These are pH-independent, electrogenic, and polyspecific transporters (14, 42). These transporters accept organic cations with relatively low molecular weight (type I cations), such as tetraethylammonium (TEA), as substrates (42, 43). Cimetidine, choline, dopamine, acyclovir, and zidovudine are also reported to be substrates (44–46).

OCTN OCTN1 is strongly expressed in the kidney but not in the adult liver (47). In OCTN1-expressing HEK293 cells, pH-sensitive uptake of TEA has been observed (47). An inward proton concentration gradient stimulated the efflux of TEA in OCTN1-expressing *Xenopus leavis* oocytes, indicating that OCTN1-mediated transport couples with proton antiport (48). OCTN1 is considered to be localized on the brush border membrane of the kidney. Substrates include quinidine and adriamycin as well as TEA (47, 48). OCTN2, an isoform of OCTN1, was isolated from human placenta and it was also found to be expressed in the kidney (49, 50). Although OCTN2 accepts TEA as its substrate, the transporter activity is not as high as that of OCTN1. OCTN2 can also accept carnitine, a zwitterion that is a cofactor essential for β-oxidation of fatty acids, and several mutations in mRNA encoding OCTN2 result in systemic carnitine deficiency owing to the poor renal reabsorption of carnitine (51). This fact suggests that OCTN2 plays a role in the renal reabsorption of carnitine. This transporter also accepts cephaloridine and other cationic compounds, such as verapamil, quinidine, and phyrilamine, in addition to TEA and carnitine, although it is not yet known whether this transporter takes part in the renal reabsorption and/or excretion of these compounds together with OCTN1 (52, 53).

Transporters in the Liver

Figure 4 shows transporters in the liver. In the liver, uptake transporters are located on the sinusoidal membrane (blood side) and efflux transporters are found on the bile canalicular membrane, although some efflux transporters are on the sinusoidal membrane and take part in the secretion into the blood.

ORGANIC ANION TRANSPORTING POLYPEPTIDES In the liver, the uptake of many organic anions is mediated by organic anion transporting polypeptides (OATPs), although OAT2 and 5 are also reported to be expressed in the liver. In humans, OATP-A, B, C, D, E, F, and 8 have been identified, and OATP-B, C and 8 are expressed in the liver (54–58). In rats, the OATP family is also conserved and Oatp1, 2, and 4 are expressed in the liver (59–61). These transporters are localized on the sinusoidal membrane of the liver. OATPs mainly accept bulky and amphipathic organic anions as substrates, although they also accept neutral compounds such as digoxin. The substrates of OATP family transporters include therapeutic drugs such as HMG-CoA reductase inhibitors, ACE inhibitors [enalapril and temocaprilat (an active form of temocapril)], and digoxin (55, 56, 58, 62–65). Many other therapeutic drugs also interact with OATP family transporters as inhibitors,

5 Oct 2004 :1308 AR AR232-PA45-28.tex XMLPublish^{SM}(2004/02/24) P1: JRX
AR REVIEWS IN ADVANCE10.1146/annurev.pharmtox.44.101802.121444

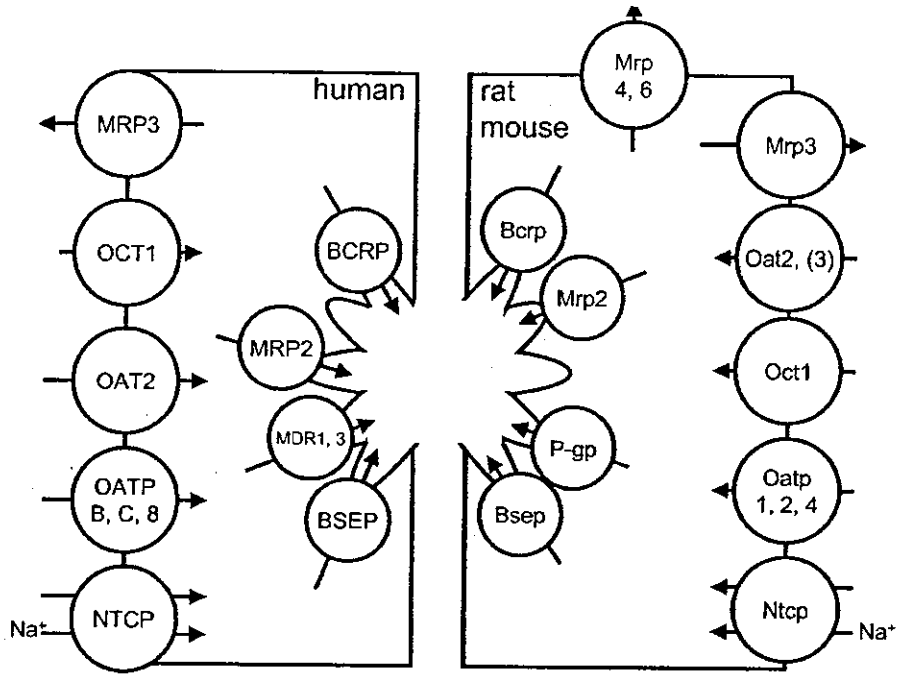

Figure 4 Transporters in the liver. Transporters expressed in human and rodent liver are summarized in this figure. Some of the transporters in rodents are expressed only in either rats or mice.

suggesting there may be other drugs that are taken up into the liver via OATP family transporters.

MULTIDRUG RESISTANCE ASSOCIATED PROTEINS In TR$^-$ and Eisai hyperbilirubinemic rats (EHBRs), which exhibit hyperbilirubinemia owing to a deficiency in the biliary excretion of bilirubin glucuronide, mutations in the transporter, multidrug resistance associated protein 2 (Mrp2), have been found (66, 67). This finding and the comparison of the biliary excretion of several compounds between normal rats and Mrp2-deficient rats suggested that it played an important role in the biliary excretion of multispecific organic anions, including glucuronide conjugates [bilirubin glucuronide, E3040 glucuronide, estradiol 17β-D-glucuronide ($E_2$17βG), grepafloxacin glucuronide, SN-38 glucuronide, glycyrrhizin, etc.], glutathione conjugate [glutathione bimane (GSB), dinitrophenyl glutathione (DNP-SG), leucotrienes (LTC_4, D_4 and E_4), etc.], grepafloxacine, MTX, pravastatin, SN-38, and temocaprilat (8, 68–72). This transporter is localized in the bile canalicular membrane of the liver (73–75). Its human counterpart (MRP2) has been isolated from the cisplatin-resistant tumor cells, KCP4 (76). This transporter is

5 Oct 2004 :1308 AR AR232-PA45-28.tex XMLPublish^{SM}(2004/02/24) P1: JRX
AR REVIEWS IN ADVANCE10.1146/annurev.pharmtox.44.101802.121444

also localized on the bile canalicular membrane of the liver and accepts multiple organic anions, including glucuronides (bilirubin monoglucuronide, bilirubin bisglucuronide, E3040 glucuronide, $E_2 17\beta G$, grepafloxacin glucuronide, LTC_4, etc.), glutathione conjugates (DNP-SG, GSB, glutathione-methylfluorescein, etc.), pravastatin, MTX, vinblastine, vincristine, etoposide, etc. (33, 77–88).

Human MRP3 is also a MRP family transporter, which is expressed in the liver. However, this transporter is localized on the sinusoidal membrane and considered to be involved in secretion into the blood. It also accepts many glucuronides, glutathione conjugates, MTX, etc. (89, 90).

BREAST CANCER RESISTANT PROTEIN Breast cancer resistant protein (BCRP) has been cloned from human MCF-7 breast cancer cells as a multidrug resistance transporter (91–93). This transporter also belongs to the ABC transporter family (91–93). However, its structure differs from that of other ABC transporters, such as MDR1 and MRP, which contain two tandem repeats of transmembrane and ABC domains. BCRP consists of only one ABC and one transmembrane domain, and, therefore, it is referred to as a half-sized ABC transporter (91–93). This transporter is also expressed in normal tissues including the liver (94). In the liver, it is located on the bile canalicular membrane (94). Many sulfated conjugates, such as estrone 3-sulfate (E_1S), dehydroepiandrosterone sulfate, 4-methylumbelliferone sulfate, etc., are transported by BCRP (95). MTX, estradiol 17β-D-glucuronide, and 2,4-dinitrophenyl-S-glutathione are also transported but to a lesser extent compared with E_1S (95). BCRP preferentially transports sulfate conjugates (95).

METHODS FOR EVALUATING TRANSPORTER-MEDIATED DRUG-DRUG INTERACTIONS IN THE KIDNEY AND THE LIVER

In Vitro Transport Systems Using Tissues, Cells, Membrane Vesicles, and Transporter-Expressing Systems

In vitro studies using tissues, cells, and membrane vesicles prepared from animals have made it easy to characterize the mechanism of drug transport and estimate the elimination rates of drugs via liver or kidney. Recently, these systems prepared from human sources have also become available, and they are likely to be of great help in the drug discovery and other related research areas. Transporter cDNA-transfected cells or cRNA-injected oocytes are also available for drug transport studies. Because of the scarcity of human tissue sources, transporter-expressing systems will be useful for predicting transporter-mediated drug-drug interactions.

KIDNEY SLICES Kidney slices were used for the study to evaluate the renal uptake of compounds/drugs from the basolateral side (96–99). In rat kidney slices, the

uptake of compounds via Oct2, Oat1, Oat3, and a novel peptide transporter has been observed (96–99). The uptake of compounds into kidney slices is much lower than the renal intrinsic uptake clearance in vivo, which may be partly due to diffusion from the surface of the slices. Although extrapolation of the renal clearance using kidney slices has not been reported, it may be used as a tool for the prediction of transporter-mediated drug-drug interactions in the kidney. At the time of writing, there have been no reports using human kidney slices; however, the use of this tool will be useful for the prediction of transporter-mediated drug-drug interactions in the kidney.

ISOLATED AND CULTURED HEPATOCYTES Isolated and cultured hepatocytes have been used as an in vitro model of the liver (100, 101). The hepatic uptake of peptidic endothelin antagonists using isolated rat hepatocytes showed that their in vitro uptake clearance could be extrapolated to give their in vivo uptake clearance, assuming a well-stirred model (100). Thus, isolated hepatocytes are a good tool for the evaluation of drug uptake in the liver and transporter-mediated drug-drug interactions in the liver. Recently, because of the progress in the techniques of cryopreservation, it seems possible to preserve frozen human hepatocytes in such a way that most of their enzymatic activity is retained (102). They have been used to examine drug metabolism interactions, including induction of metabolic enzymes (103–105). Recently, we have examined the uptake of taurocholate (TC) and estradiol-17β-D-glucuronide in freshly-isolated and cryopreserved human hepatocytes (106). This study suggested that their active transports were retained even in cryopreserved human hepatocytes, although the activity was decreased after cryopreservation in some lots of hepatocytes (106). Therefore, cryopreserved human hepatocytes, at least, retain transporter function and they can be used as a useful experimental system for examining the mechanism of the hepatic uptake of drugs and interactions with other drugs (106).

LIVER SLICES Liver slices are also used for the study of drug uptake in the liver (107, 108). Olinga et al. examined the uptake of digoxin, a substrate of human OATP8 [OATP1B3] and rat Oatp2 [Oatp1a4], and temperature-dependent uptake was observed (107). Liver slices are supplemented with nonparenchymal cells, and, therefore, the interaction between hepatocytes and other cells and the effect of other cells on the function of hepatocytes can also be examined.

MEMBRANE VESICLES Today, membrane vesicles prepared from the brush border and basolateral membrane in the kidney and from the sinusoidal and bile canalicular membrane in the liver are readily available for the study of renal and hepatobiliary transport (109–114). The advantages of using this system for transport studies are (*a*) drug transport across the basolateral (sinusoidal) and apical (brush border or bile canalicular) membrane can be measured separately, (*b*) intracellular binding and/or metabolism can be ignored, and (*c*) buffers inside and outside vesicles can be changed easily. On the other hand, using this system has limitations because it

5 Oct 2004 :1308 AR AR232-PA45-28.tex XMLPublish^{SM}(2004/02/24) P1: JRX
AR REVIEWS IN ADVANCE10.1146/annurev.pharmtox.44.101802.121444

requires a driving force for transport, so it is impossible to use this system without prior characterization.

STUDIES USING GENE EXPRESSION SYSTEMS Using transporter expression systems, the kinetic parameters for the target transporter can be obtained. Once the responsible transporter for the drugs in question has been identified, the possibility of drug-drug interactions can be examined using the gene expression system, i.e., without hepatocytes, membrane vesicles, and tissue slices. As human tissue samples are scarcely distributed, transporter-expressing systems greatly help drug transport studies. With the information of contributions of specific transporter(s) to the total uptake of drugs in human liver or kidney, quantitative prediction of drug uptake in human tissues is possible. The method to estimate the contributions of specific transporters is described below. cDNA-transfected cells and cRNA-injected oocytes can be used as gene expression systems. More recently, cultured cells stably transfected with both uptake and efflux transporters have become available (85, 115). OATP-C/OATP2 [OATP1B1] and MRP2 transfected cells and OATP8 [OATP1B3] and MRP2 transfected cells have been reported (Figure 5) (85, 115). Using them, hepatobiliary transport can be measured as vectorial transcellular transport when these cells are cultured on a porous membrane. This will make it easy to predict transporter-mediated drug-drug interactions in the liver.

ESTIMATION OF THE CONTRIBUTION OF A SPECIFIC TRANSPORTER The estimation of the contribution of specific transporter(s) is important for the quantitative prediction of the uptake in human tissues, including liver and kidney from the in vitro data using transporter-expressing systems, and even for the quantitative

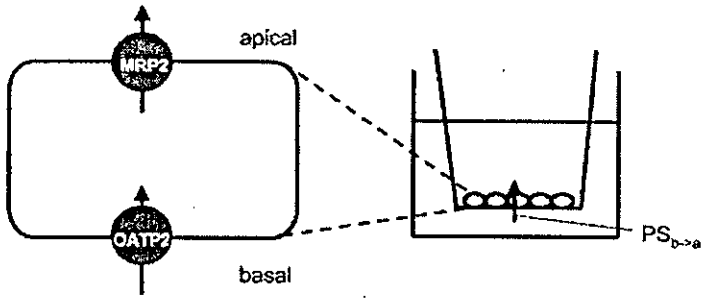

Figure 5 Experimental system for the estimation of transcellular transport of drugs mediated by OATP-C/OATP2 [OATP1B1] and MRP2. OATP-C/OATP2 [OATP1B1] and MRP2 double-transfected MDCK cells are seeded in a membrane insert. The basal-to-apical flux of drugs across the MDCK cell monolayer was examined to estimate the transcellular transport mediated by OATP-C/OATP2 [OATP1B1] and MRP2.

prediction of transporter-mediated drug-drug interaction. Here, we show the method to estimate it in in vitro assays.

First, injection of cRNA coding a transporter results in its expression on the plasma membrane of *Xenopus laevis* oocytes that have been used for expression cloning, functional analysis, or transport assays (117, 118). However, hybridization of mRNA with antisense oligonucleotide coding a specific sequence for the target transporter specifically reduces the expression of the transporter (117, 118). Comparison of the transporter activity in cRNA-injected oocytes in the presence and absence of antisense nucleotides gives the contribution of each transporter to the net transport (117, 118).

Kouzuki et al. have proposed a method using reference compounds (119, 120). They measured the uptake of reference and test compounds at the same time in transporter cDNA-transfected COS7 cells and rat hepatocytes and calculated the contribution using the following equation (119, 120):

$$\text{Contribution} = \frac{CL_{hep,ref}/CL_{COS,ref}}{CL_{hep,test}/CL_{COS,test}}, \quad (6)$$

where CL_{hep} and CL_{COS} represent the uptake clearance of compounds into hepatocytes and transporter cDNA transfected cells, respectively. $CL_{\#,ref}$ and $CL_{\#,test}$ represent the uptake clearance of the reference and test compounds, respectively. The reference compounds should be specific substrates, otherwise the contribution will be overestimated (119, 120). More recently, Hirano et al. proposed a method to estimate the contributions of human transporters (OATP-C/OATP2 [OATP1B1] and OATP8 [OATP1B3]) to the total hepatic uptake using estrone 3-sulfate and cholecystokinine octapeptide (CCK8) as specific substrates, respectively, and actually estimated their contributions to the hepatic uptake of pitavastatin (121). They also estimated their contributions by uptake in human hepatocytes and transporter expression systems normalized by their transporter expression levels measured by Western blot analysis (121). The contributions of OATP-C/OATP2 [OATP1B1] and OATP8 [OATP1B3] estimated by these two different methods were comparable, suggesting the validity of this method (121).

A specific inhibitor of a transporter also helps to estimate its contribution to the total uptake. To identify a specific inhibitor, we examined the comparative inhibitory effects of many compounds on rat Oatp1 [Oatp1a1] and Oatp2 [Oatp1a4] (122). Among them, we found that digoxin specifically inhibited Oatp2 [Oatp1a4] with no effect on Oatp1 [Oatp1a1] (122). We also found several compounds which preferentially inhibited one of these transporters (122). These inhibitors may be used to estimate the contributions of Oatp1 [Oatp1a1] and Oatp2 [Oatp1a4] at appropriate concentrations (122). However, the selectivity of most of the preferential inhibitors in this report was not very high, and inhibitors that act as selective inhibitors over a wider range of concentrations are needed (122).

5 Oct 2004 :1308 AR AR232-PA45-28.tex XMLPublish^{SM}(2004/02/24) P1: JRX
AR REVIEWS IN ADVANCE10.1146/annurev.pharmtox.44.101802.121444

EVALUATION OF TRANSPORTER-MEDIATED DRUG-DRUG INTERACTIONS

In this section, the inhibitory effects of therapeutic drugs and the possibility of clinically relevant drug-drug interactions based on transporter-mediated processes are described.

How to Evaluate the Extent of Transporter-Mediated Drug-Drug Interactions

Previously, our group has suggested how to predict the extent of drug-drug interactions based on drug metabolism using in vitro studies (123, 124). This method can also be applied to transporter-mediated drug-drug interactions (125). As transporter-mediated influx or efflux follows the Michaelis-Menten equation, the clearance can be described as follows:

$$CL = \frac{V_{max}}{K_m + S_u} + P_{dif}, \quad (7)$$

where CL is the influx or efflux clearance; V_{max}, K_m, and P_{dif} are the maximum transport rate, Michaelis constant, and nonsaturable transport clearance, respectively; and S_u is the protein-unbound substrate concentration. In the presence of competitive inhibitors, it can be described as follows:

$$CL(+\text{inhibitor}) = \frac{V_{max}}{K_m \cdot (1 + I_u/K_i) + S_u + P_{dif}}, \quad (8)$$

where I_u is the protein-unbound inhibitor concentration and K_i is the inhibition constant. It should be noted that the I_u value is the protein-unbound inhibitor concentration outside the cells for influx transporters, whereas it is that inside the cells for efflux transporters. On the other hand, in the case of noncompetitive inhibition, it can be described as follows:

$$CL(+\text{inhibitor}) = \frac{V_{max}/(1 + I_u/K_i)}{K_m + S_u} + P_{dif}. \quad (9)$$

When the protein unbound substrate concentration is negligibly low compared with the K_m value, the influx or efflux clearance via transporters can be described by the following equation, both for competitive and noncompetitive inhibition:

$$CL(+\text{inhibitor}) = \frac{V_{max}}{K_m \cdot (1 + I_u/K_i)} + P_{dif}. \quad (10)$$

Therefore, transporter-mediated influx or efflux clearance (i.e., net influx or efflux clearance subtracted by the nonsaturable clearance) is decreased by the following equation:

$$\frac{CL_{transporter}\,(+inhibitor)}{CL_{transporter}\,(control)} = \frac{1}{1 + I_u/K_i} = R, \tag{11}$$

where $CL_{transporter}$ represents transporter-mediated influx or efflux clearance.

When a transporter, which is a key determinant of the disposition of a drug, is inhibited by a concomitantly administered drug, the area under the blood/plasma concentration (AUC) after an oral administration will increase by at most $\frac{1}{R}$-fold when the drug is predominantly excreted in the liver. In such cases, hepatic or renal intrinsic clearances decrease by R-fold and, therefore, this R value is one of the indicators of the severity of a drug-drug interaction. It should be particularly useful for the evaluation of in vivo drug-drug interactions to avoid false negative predictions.

For the liver transporters, the estimation of I_u should account for the inhibitors in the portal vein as well as the hepatic artery when the inhibitor drug is orally administered. In this case, I_u is not equal to the inhibitor concentration in the circulating blood. Ito et al. have suggested a method to estimate the inhibitor concentration at the inlet to the liver using the following equation (Figure 6) (123, 124):

$$I_u = f_u \cdot (I_{sys} + I_{pv}) = f_u \cdot \left(I_{sys} + \frac{v_{abs}}{Q_H}\right), \tag{12}$$

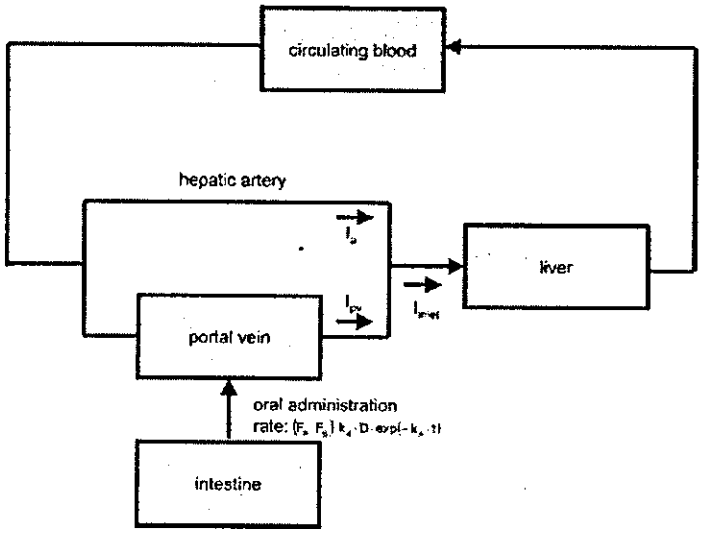

Figure 6 A model for estimating the inhibitor concentration at the inlet to the liver after oral administration. I_{inlet} is the inhibitor concentration at the inlet to the liver. It can be estimated from the inhibitor concentration in the hepatic artery (I_a) plus that in the portal vein (I_{pv}).